ELSEVIER

Thermochimica Acta 387 (2002) 39–45

thermochimica acta

www.elsevier.com/locate/tca

Thermal and structural characterization of trimethylolethane trihydrate

M. Yamazaki[a,*], C. Sasaki[b], H. Kakiuchi[a], Y.T. Osano[b], H. Suga[c]

[a]*Mitsubishi Chemical Co. Ltd., Tsukuba Research Center, 8-3-1 Ami, Ibaraki 300-0332, Japan*
[b]*Mitsubishi Chemical Co. Ltd., Yokohama Research Center, 1000 Kamoshida, Yokohama 227-8502, Kanagawa, Japan*
[c]*Research Institute for Science and Technology, Kinki University, Kowakae, Higashi-Osaka 577-8502, Japan*

Received 24 June 2001; received in revised form 10 October 2001; accepted 17 October 2001

Abstract

Differential scanning calorimetry (DSC) was used to determine the phase diagram of the binary system, trimethyloloethane (TME) + water; a system of interest in relation to latent heat storage organic hydrate materials. A stable hydrate was formed between the two components. The hydrate melted incongruently at 303.0 K with a latent heat of 218 kJ kg^{-1}. The eutectic point between the hydrate and ice was observed at 271.1 K. The composition of the hydrate estimated from the peak area of the eutectic melting was 3 mol of water against 1 mol of TME. Since this composition of the hydrate was different from that reported in literature, a new sample of the hydrate was prepared. After careful drying of the hydrate, gravimetric analysis gave the stoichiometric amount of water to be (3.00 ± 0.01). From a single crystal X-ray structural analysis, it was found that the hydrate crystal had a layered structure with alternate TME and water layers. Each TME layer was linked by hydrogen bonding through the water layer. In an asymmetric unit there was one TME molecule, and the oxygen atoms of the water molecules were statistically located on five positions with occupancy factor of 1.0, 1.0, 0.5, 0.25, and 0.25, respectively. Therefore, the stoichiometric amount of water against one TME molecule is 3. Hence, the X-ray diffraction confirmed the proposed hydration number of the stable hydrate.

Keywords: Trimethylolethane trihydrate; Phase diagram; Crystal structure; Latent heat; Storage material

1. Introduction

In recent years, there has been an increased interest in latent heat storage techniques related to advanced utilization of energy. A wide variety of liquid and solid materials suitable at different application temperatures have been proposed [1–4]. Typical examples are water, sodium acetate trihydrate, calcium chloride hexahydrate, and sodium sulfate decahydrate. A special container is required for the purpose. The container must be resistive against corrosion by the involved ions and furthermore withstand the volume change on melting. Phase separation of some materials is another problem to be solved. Paraffin is an organic latent heat storage material of relatively low working temperature. Although paraffin is free from the above problems, high purity samples must be used in order to have a sharp process in cases where a fast melting–crystallization cycle is requested. This situation results in a high performance cost. Organic hydrates may replace paraffin, but few investigations have been reported.

* Corresponding author. Fax: +81-298-87-4447.
E-mail address: 3805864@cc.m-kagaku.co.jp (M. Yamazaki).

0040-6031/02/$ – see front matter
PII: S0040-6031(01)00821-8

Solid–solid transitions with a large latent heat can also be used for the heat reservoir. Pentaerythritol and homologous series of polyols, $(CH_3)_{4-n}C(CH_2OH)_n$, are good examples [5]. The transition mechanism has been discussed based on conformational changes of molecules induced by breaking the intermolecular hydrogen bond [6]. The transition temperature increases systematically with n, while the enthalpy of transition is roughly proportional to n^2 [5]. Thus, 2-hydroxymethyl-2-methyl-1,3-propanediol with $n=3$ (commonly designated as trimethylolethane (TME)) undergoes a solid–solid transition at 354 K with the associated enthalpy change of 23.1 kJ mol^{-1}. Accordingly, these substances attracted notice as latent heat storage materials at high temperatures [7–11]. Interestingly, when we prepared TME aqueous solution, the substance was found to form a stable hydrate. Benson and Burrows [12] applied for a patent covering a whole range of possible hydrates TME·xH_2O with $1 < x < 20$. Laugt and Teisseire [13] reported later that there was only one stable hydrate and that the composition was TME·$4H_2O$, i.e. tetrahydrate. The number of crystal water was determined by elemental analysis of the crystal. They also analyzed the X-ray diffraction patterns of the hydrate at room temperature and determined the space group to be $I4_1/a$ (tetragonal) and the unit cell size as $a = 9.102$ Å, $c = 47.654$ Å. The hydrate TME·$4H_2O$ is the most efficient latent heat storage material in the binary system TME + H_2O.

We have studied the phase diagram of the same system; TME + H_2O. Unexpectedly, the hydration number of the stable hydrate was determined to be 3. The preparation of the hydrate reported in the study by the previous workers may be questioned. These authors [13] have reported that the crystal was of effloresent nature and care was taken to keep the surface transparent by maintaining the sample in a water-saturated air atmosphere. Hence, there might be a possibility that the sample includes some mother liquid. We have prepared the hydrate and determined gravimetrically the hydration number to be (3.00 ± 0.01). Some preliminary results including the thermal stability of the hydrate have been reported [14]. Experimental details of the analysis are described in the present paper. A preliminary X-ray structural analysis of the trihydrate is also reported.

2. Experimental

Reagent grade trimethylolethane was purchased from Wako Pure Chemical Industries in Japan and used without purification. The only impurity that influences on experiments is residual moisture in the sample. In view of hygroscopic nature of the polyols, small amount of moisture will affect seriously the water content of the samples in the study of the phase diagram. Thus, the samples were pulverized and kept in a desiccator over silica gel for a long time.

For the determination of the hydration number of hydrate formed, the sample was purified first by recrystallization from a methanol solution, followed by sublimation in vacuo at elevated temperatures. The preparation of the stable hydrate and the method used to accurately determine the water content will be described later.

DSC experiments were carried out with a Model 220C manufactured by Seiko Instrument in Japan. Samples with various compositions were prepared gravimetrically from TME crystal and distilled water, and each sample of 2–3 mg was sealed in an aluminum pan. Efforts were paid particularly to the homogenization of composition. A sample pan was heated with the rate of 5 K min^{-1} from 293 to 320 K and held at the temperature for 10 min. After cooling it with the rate of 5 K min^{-1} from 320 to 278 K, the pan was held at that temperature for 10 min. Then the sample pan was cooled from 278 to 263 K, followed by a further cooling from 263 to 243 K in the same stepwise manner. A heating run with the rate of 2 K min^{-1} was subsequently started and the peaks observed during the run were used to construct the phase diagram. When the TME concentration in the solution was very low, the DSC measurements were carried out at 0.1 K min^{-1} of heating rate (to detect the eutectic temperature).

X-ray structural analysis of the hydrate was done using Model SMART 1000 CCD system made by Bruker in Germany. X-ray beam from Mo Kα and a single crystal of 0.7 mm × 0.7 mm × 0.2 mm dimension were used for the diffraction experiment. The crystal was coated with paraffin oil for protecting the sample from dehydration and flash cooled by N_2 gas stream from a cryostat to 110 K. All diffraction data was collected at 110 K.

3. Results and discussion

3.1. Phase diagram

Typical DSC curves are given in Fig. 1 for selected compositions. The curves show peaks associated with a eutectic melting and the subsequent dissolution of remaining crystal. The eutectic temperature was taken as the onset point of the curve, while the peak point was used for the liquidus temperature. The points were plotted as a function of mole fraction of TME, x_{TME}, for the construction of the phase diagram. The results are drawn in Fig. 2. The diagram indicates clearly the existence of a stable hydrate that undergoes an incongruent melting at 303.0 K. The associated enthalpy change is 218 kJ mol^{-1}. As shown in Fig. 2, TME hydrate and TME anhydride crystal coexist at the composition of $x = 0.25$. Thus, after the complete TME hydrate melted, the dissolution peak of TME anhydride crystal was observed at around 310 K. The eutectic point between ice and the hydrate crystals was found at 271.1 K. In order to determine the composition of the eutectic mixture and the stable hydrate, the enthalpy change at the eutectic temperature was plotted, as a function of mole fraction x_{TME}, see Fig. 3.

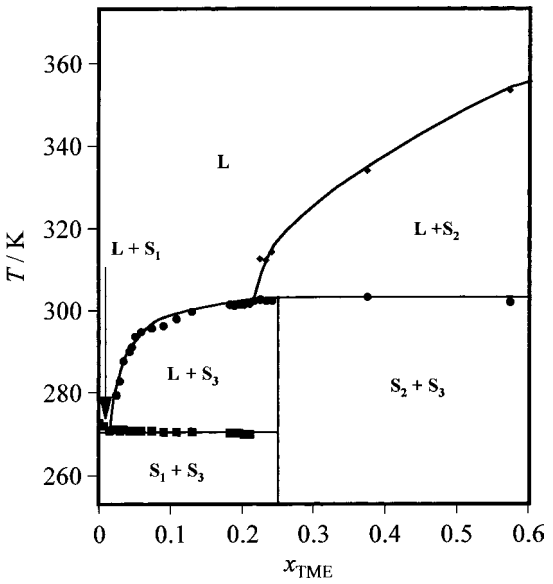

Fig. 2. The phase diagram of TME and water determined by DSC measurements: L, liquid; S1, ice; S2, TME; S3, TME trihydrate.

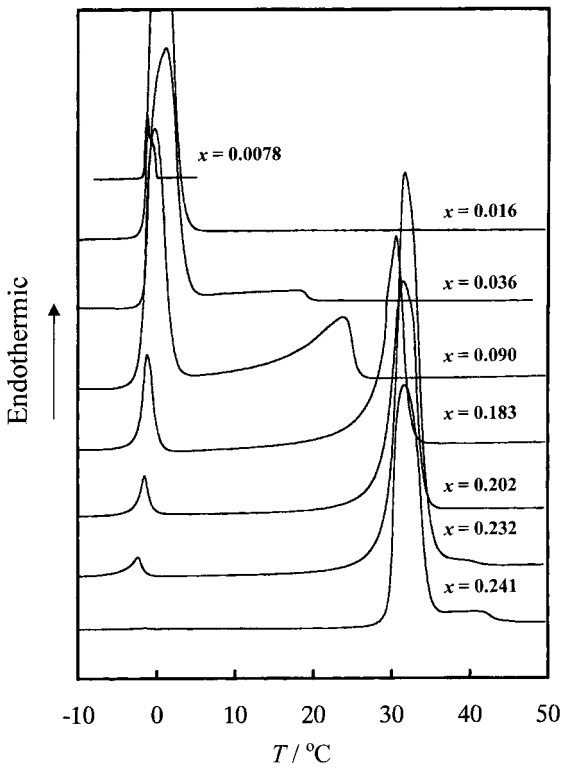

Fig. 1. Typical DSC curves for selected compositions.

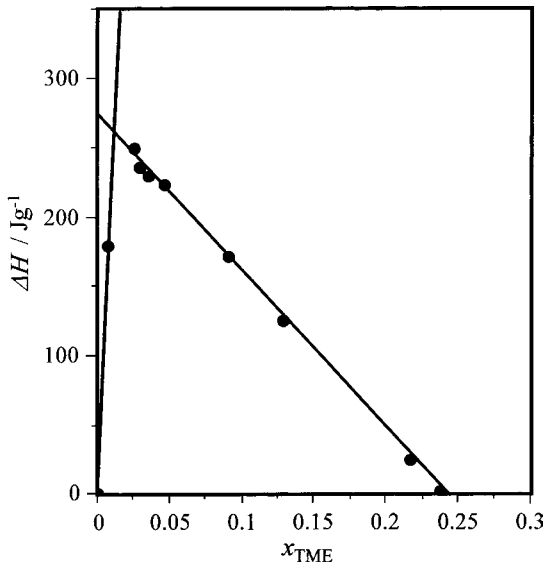

Fig. 3. The relations between the enthalpy and TME concentrations calculated by the changes in eutectic peak area in the DSC experiments.

Table 1
The results of the determination of water in TME hydrate

	TME hydrate (g)	After drying (g)	Mass reduction (g)	Hydration number
1	0.0509	0.0351	0.0158	3.0003
2	0.0950	0.0655	0.0295	3.0019
3	0.1621	0.1117	0.0504	3.0074

Table 2
Basic thermal properties of TME hydrate

Melting point (K)	303
Heat of fusion (kJ kg^{-1})	218
Specific heat (kJ kg^{-1} K^{-1})	
283 K	2.75
323 K	3.58
Density (g dm^{-3})	
283 K	1.12
323 K	1.09
Heat conductivity (W m^{-1} K^{-1})	
295 K	0.65
329 K	0.21

Table 3
Atomic coordinates and equivalent isotropic displacements parameter ($Å \times 10^3$) for TME hydrate

	x	y	z	U(eq)[a]	s.o.f[b]
O(2)	0.4797(4)	0.4929(5)	0.0415(1)	32(1)	1.000
O(3)	1.0195(4)	0.4928(5)	0.0398(1)	31(1)	1.000
C(1)	0.7501(6)	0.4758(6)	0.0415(1)	23(1)	0.944
C(2)	0.6146(6)	0.5742(6)	0.0381(1)	26(1)	0.944
C(3)	0.8854(5)	0.5756(6)	0.0381(1)	23(1)	0.944
C(4)	0.7491(7)	0.3538(7)	0.0185(1)	27(1)	0.944
O(4)	0.7484(6)	0.4098(6)	−0.0100(1)	36(1)	0.944
C(5)	0.7508(7)	0.3982(7)	0.0705(1)	29(1)	0.944
C(1′)	0.7620(5)	0.5280(7)	0.0414(16)	30	0.056
C(2′)[c]	0.6244	0.4303	0.0384	30	0.056
C(3′)	0.8840(4)	0.4130(8)	0.0370(2)	30	0.056
C(4′)	0.7410(12)	0.6440(9)	0.0179(12)	30	0.056
O(4′)	0.7340(8)	0.6060(9)	−0.0118(13)	30	0.056
C(5′)	0.7590(1)	0.5940(12)	0.0715(17)	30	0.056
OW1	1.01006(4)	0.4958(5)	0.0959(1)	26(1)	1.000
OW2	0.4018(4)	0.4957(5)	0.0977(1)	28(1)	1.000
OW3[d]	1.0000	0.7500	0.1225(1)	27(1)	0.500
OW4[d]	1.0000	0.2500	0.1250	27(2)	0.250
OW5[d]	0.5000	0.7500	0.1250	35(2)	0.250

[a] U(eq) is defined as one-third of the trace of the orthogonalized U_{ij} tensor.
[b] Site occupancy factor.
[c] The position of C(2′) was fixed to refine structure.
[d] OW3, OW4 and OW5 are on special position. OW3 on inversion center, OW4 and OW5 on four-fold axis.

To our surprise, the composition of the hydrate turned out to be close to TME trihydrate ($x_{TME} = 0.25$) rather than TME tetrahydrate ($x_{TME} = 0.20$) reported earlier by Laugt and Teisseire [13]. The determination of the exact hydration number of the hydrate is important in the practical use of latent heat storage materials, since the existence of excess water diminishes the enthalpy of fusion. For this purpose, a new sample of the hydrate was prepared by using the phase equilibrium between the hydrates and anhydride crystals of TME when stored in a desiccator. These samples was subsequently subjected to gravimetric analysis.

3.2. Determination of hydration number

The determination of the hydration number of the hydrate crystal was initiated by purification of the

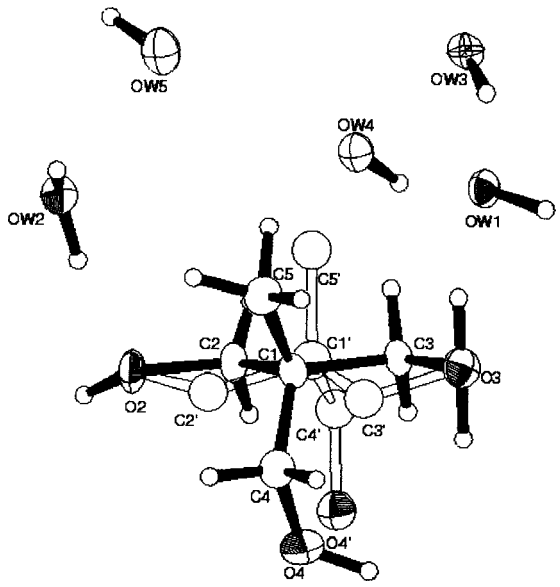

Fig. 4. The structure of the TME trihydrate, 50% probability displacement ellipsoids and atom-numbering scheme. Hydrogen atoms are shown as shares of arbitrary radii.

TME crystal in order to eliminate the effect of impurities involved in the original sample. The crystal was purified by recrystallization from a methanol solution and subsequent sublimation in vacuo at elevated temperatures, as stated earlier. Sublimation is particularly necessary in order to remove the trapped water inside the polyols crystals, as has been described in detail for pentaerythritol [15]. The process destructs the crystalline lattice and extracts the constituents in molecule-by-molecule fashion. This method is one of the best ways for efficient removal of residual water absorbed tightly inside strongly hydrophilic crystals.

The purified TME was dissolved in hot distilled water. Highly efflorescent hydrate was obtained easily by cooling of the solution. The crystal including mother liquid was stored with a mixture of the hydrate and anhydride crystals. The amount of the anhydride crystals should be sufficient to absorb the excess water. As long as the mixtures of crystals were present, the space inside the desiccator can keep the equilibrium saturation vapor pressure of the hydrate. The desiccator was kept at 300 K until the thermal equilibrium inside the vessel was established. Excess water is absorbed by anhydride crystals until the equilibrated composition of the hydrate is realized. The thermal equilibrium can be examined by measuring the sample mass, which became almost constant after 2 weeks. Since interior excess water molecules will diffuse out slowly, the desiccator was kept for further 2 weeks to secure a good product.

The hydrate crystal prepared by the method given above was weighed and desiccated over silica gel in an evacuated vessel until the dehydration is completed. Three gravimetric analyses are summarized in Table 1. The results show that the hydration number is 3.003 ± 0.010. Thus, the correct composition is TME trihydrate.

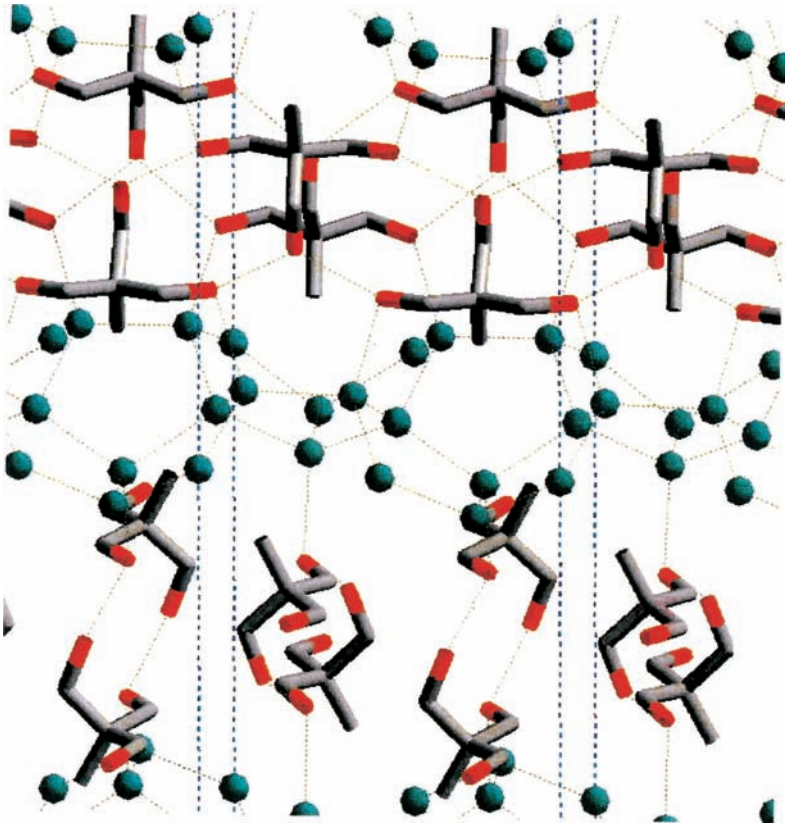

Fig. 5. The hydrogen bonds networks in the TME hydrate. Gray, Red and Green balls represent carbon, oxygen disordered parts of TME hydrate and oxygen of water molecules, respectively. Green broken lines represent hydrogen bonds.

3.3. Basic physical properties of TME trihydrate

The basic physical properties of TME trihydrate thus determined are summarized in Table 2. The temperature and enthalpy of fusion of the crystal were determined by the present DSC measurement. Specific heat capacity was determined by the Agune Technical Center in Japan using DSC-7 produced by Perkin-Elmer Co. Ltd. Thermal conductivity was measured by Shinku-Riko Inc. model TH-1000 using a hot-wire method. Density was measured by using an Archimedes principle. The hydrate has an enthalpy of fusion of about 218 kJ kg^{-1} and a density more than 1. Because of its large latent heat of fusion per unit volume, the hydrate must be seen as a promising latent heat storage material for the relatively low temperature range.

3.4. X-ray structural analysis

Since Laugt and Teisseire [13] have determined only the space group and lattice constants of the hydrate crystal, we carried out X-ray structural analysis of the trihydrate to elucidate the structure of the TME molecule and the positions of water molecules in the lattice. The main crystallographic parameters are following.; tetragonal, space group $I4_1/a$ $a = 9.046$ (9) Å, $c = 46.718$ (4) Å, $V = 3823$ (5) $Å^3$, $Z = 16$. The numerical value in parentheses is standard deviation. In an asymmetric unit there was one TME molecule, and the oxygen atoms of the water molecules were statistically located on five positions with occupancy factor of 1.0, 1.0, 0.5, 0.25 and 0.25, respectively. Therefore, the hydration number relative

Table 4
Hydrogen bond lists for one TME molecule

Donor	Acceptor	Symmetry operation	Distance (Å)
O2(TME)	O4	$1.000 - X, 1.000 - Y, 0.000 - Z$	2.67
	O4′	$1.000 - X, 1.000 - Y, 0.000 - Z$	2.54
	OW2	$0.000 + X, 0.000 + Y, 0.000 + Z$	2.72
O3(TME)	O4	$2.000 - X, 1.000 - Y, 0.000 - Z$	2.67
	O4′	$2.000 - X, 1.000 - Y, 0.000 - Z$	2.74
	OW1	$0.000 + X, 0.000 + Y, 0.000 + Z$	2.72
O4(TME)	O2	$1.000 - X, 1.000 - Y, 0.000 - Z$	2.69
	O3	$2.000 - X, 1.000 - Y, 0.000 - Z$	2.67
	O4′	$0.000 + X, -0.500 + Y, 0.000 - Z$	2.94
O4′(TME)	O2	$1.000 - X, 1.000 - Y, 0.000 - Z$	2.54
	O3	$2.000 - X, 1.000 - Y, 0.000 - Z$	2.74
	O4	$0.000 + X, 0.500 + Y, 0.000 - Z$	2.94
OW1(Water)	O3	$0.000 + X, 0.000 + Y, 0.000 + Z$	2.72
	OW2	$1.000 + X, 0.000 + Y, 0.000 + Z$	2.73
	OW3	$0.000 + X, 0.000 + Y, 0.000 + Z$	2.77
	OW4	$0.000 + X, 0.000 + Y, 0.000 + Z$	2.76
OW2(Water)	O2	$0.000 + X, 0.000 + Y, 0.000 + Z$	2.72
	OW1	$-1.000 + X, 0.000 + Y, 0.000 + Z$	2.73
	OW3	$-0.250 + Y, 1.250 - X, 0.250 - Z$	2.77
	OW5	$0.000 + X, 0.000 + Y, 0.000 + Z$	2.78
OW3(Water)	OW1	$0.000 + X, 0.000 + Y, 0.000 + Z$	2.77
	OW1	$2.000 - X, 1.500 - Y, 0.000 + Z$	2.77
	OW2	$0.750 + Y, 1.250 - X, 0.250 - Z$	2.77
	OW2	$1.250 - Y, 0.250 + X, 0.250 - Z$	2.77
OW4(Water)	OW1	$0.000 + X, 0.000 + Y, 0.000 + Z$	2.76
	OW1	$2.000 - X, 0.500 - Y, 0.000 + Z$	2.76
	OW1	$0.750 + Y, 1.250 - X, 0.250 - Z$	2.76
	OW1	$1.250 - Y, -0.750 + X, 0.250 - Z$	2.76
OW5(Water)	OW2	$0.000 + X, 0.000 + Y, 0.000 + Z$	2.78
	OW2	$1.000 - X, 1.500 - Y, 0.000 + Z$	2.78
	OW2	$-0.250 + Y, 1.250 - X, 0.250 - Z$	2.78
	OW2	$1.250 - Y, 0.250 + X, 0.250 - Z$	2.78

to one TME molecule is 3 (Table 3 and Fig. 4). The space group was determined as given above. However, the final R value ($R = 0.139$ at 223 K) was slightly large. We also carried out X-ray diffraction measurements at 110 K, but the R value ($R = 0.127$ for 1673 reflections ($I > 2\sigma(I)$)) could not be improved. As shown in Table 3 and Fig. 4, the TME molecules are disordered. Atom labels C1′, C2′, C3′, C4′, O4′ and O5′ represent disordered parts, and the site occupancy factor (s.o.f.) of disordered parts is low (0.056). The rather poor final R value is thought to be the result of this nature of the hydrate. There are no evidence for a order–disorder transition of the TME trihydrate for temperature above 110 K in the present DSC measurements. Still, TME trihydrate might undergo a ordering phase transition at temperatures below 110 K. In order to attain more definite results, neutron scattering might be useful to determine the positions of hydrogen atoms.

TME hydrate has a layer structure composed of alternating TME and water layers (Fig. 5). TME molecules were linked by hydrogen bonding between O4 and O2 of the next TME molecules ($1.00 - x$, $1.00 - y$, $0.00 - z$) and O3 ($2.00 - x$, $1.00 - y$, $0.00 - z$), and each TME layer was linked by hydrogen bonding through the water layer (Figs. 4 and 5 and Table 4). In the water layer each water molecules were linked by hydrogen bonding to the next water molecules. In Table 4, all the distance of the hydrogen bonding and the symmetric relation between donors and acceptors are shown. In this way TME molecules and water molecules make a hydrogen bond network all over the TME hydrate.

On the other hand, it is very interesting that the TME forms a hydrate. Homologous polyalcohols such as pentaerythritol and 2,2-dimethyl-1,3-propandiol do not form a hydrate. This suggests that the hydrophobic methyl group which plays a very important role to form the TME trihydrate. Also, the hydroxymethyl groups in TME molecule may be of importance.

Acknowledgements

The authors would like to express their sincere thanks to Ms. K. Yokomizo for the preparation of samples and Prof. S. Ichihara of Tokyo University of Agriculture & Technology for helpful discussion in DSC measurement and analysis.

References

[1] A. Abhat, Solar Energy 30 (1983) 313.
[2] M. Telkes, Am. Soc. Heat. Refrigerat. Air-Condition. Eng. Trans. 16 (1974) 38.
[3] H. Kimura, J. Kai, Mater. Energy-Shigen 5 (1984) 90.
[4] H. Kakiuchi, in: Proceedings of the 1994 MIE International Forum and Symposium on Global Environment and Friendly Energy Technology, Mie, Japan, 1994, p. 339.
[5] D.K. Benson, R.W. Burrows, J.D. Webb, Solar Energy Mater. 13 (1986) 133.
[6] K. Suenaga, T. Matsuo, H. Suga, Thermochim. Acta 163 (1990) 263.
[7] D.K. Benson, C. Christensen, in: Proceedings on the Passive and Hybrid Solar Energy Update, Washington, DC, 1983, p. 261.
[8] J. Font, J. Muntasell, J. Navarro, J, L.-L. Tamarit, Solar Energy Mater. 15 (1987), pages 299, 403.
[9] Y. Sakata, Y. teranuma, T. Usami, S. Chihara, H. Kakiuchi, M. Yamazaki, M. Yabe, in: Proceedings of the 34th Japanese Conference on Calorimetry and Thermal Analysis, Yokohama, Japan, 1998, p. 32.
[10] M. Yamazaki, H. Kakiuchi, M. Yabe, S. Chihara, in: Proceedings of the 63rd Spring Meeting of Society Chemical Engineering, Japan, Vol. 1, 1998, p. 189.
[11] M. Yabe, H. Kakiuchi, M. Yamazaki, S. Chihara, K. Ozaki, H. Inaba, in: Proceedings of the International Conference on Energy Storage Technologies and Systems, Indore, India, 1999, p. 11.
[12] D.K. Benson, R.W. Burrows, US Patent No. 4, 1987, 702,853.
[13] M. Laugt, M. Teisseire, Powder Diffract. 6 (1991) 190.
[14] M. Yamazaki, H. Kakiuchi, M. Yabe, S. Chihara, in: Proceedings of the 3rd International Symposium on Heating, Ventilation and Air Conditioning, China, 1999, p. 497.
[15] I. Nitta, S. Seki, M. Momotani, Proc. Jpn. Acad. 26 (1950) 11.